

Self-assembly of a model supramolecular polymer studied by replica exchange with solute tempering

Hadi H. Arefi and Takeshi Yamamoto*

Department of Chemistry, Graduate School of Science, Kyoto University, Kyoto 606-8502, Japan

Conventional molecular-dynamics (cMD) simulation has a well-known limitation in accessible time and length scales, and thus various enhanced sampling techniques have been proposed to alleviate the problem. In this paper we explore the utility of replica exchange with solute tempering (REST) (i.e., a variant of Hamiltonian replica exchange methods) to simulate the self-assembly of a supramolecular polymer in explicit solvent, and compare the performance with temperature-based replica exchange MD (T-REMD) as well as cMD. As a test system, we consider a relatively simple all-atom model of supramolecular polymerization (namely, benzene-1,3,5-tricarboxamides in methylcyclohexane solvent). Our results show that both REST and T-REMD are able to predict highly ordered polymer structures with helical H-bonding patterns, in contrast to cMD which completely fails to obtain such a structure for the present model. At the same time, we have also experienced some technical challenge (i.e., aggregation-dispersion transition and the resulting bottleneck for replica traversal), which is illustrated numerically. Since the computational cost of REST scales more moderately than T-REMD, we expect that REST will be useful for studying the self-assembly of larger systems in solution with enhanced rearrangement of monomers.

Introduction. Supramolecular polymerization, i.e., the self-assembly of monomers into one-dimensional ordered structures via non-covalent interactions, has been receiving increased attention for developing advanced functional materials.^{1–5} A variety of factors including monomer structures, environments, and their interactions play crucial roles for assembly structures and aggregation properties. To obtain more insights into their relationship, molecular-dynamics (MD) simulations have been carried out for representative systems.⁴ However, a well-known drawback of direct MD simulations (particularly based on all-atom models) is that accessible time and spatial scales are often too limited to study self-assembly processes. Therefore, various approaches have been used to alleviate the difficulty, including the use of coarse-grained models.⁶

In this paper we are interested in the utility of enhanced sampling^{7–9} for studying supramolecular polymerization. Temperature-based replica exchange MD (T-REMD)^{10,11} is among the most popular approaches for this purpose. In T-REMD, one evolves a set of replicas at different temperatures and exchanges their coordinates periodically. This facilitates the replica at the target temperature to overcome energy barriers and explore a wider conformational space.¹² Despite its utility, the computational cost of T-REMD increases with the total degrees of freedom, making it expensive to study a large system in explicit solvent. Replica exchange with solute tempering (REST)^{13–15} deals with this problem by using a modified potential energy function^{15–17}

$$E_m = \frac{\beta_m}{\beta_0} E_{uu} + \sqrt{\frac{\beta_m}{\beta_0}} E_{uv} + E_{vv}, \quad (1)$$

where E_{uu} , E_{uv} , and E_{vv} are solute-solute, solute-solvent, and solvent-solvent interaction energies, respectively, $\beta_m = 1/(k_B T_m)$ with T_m the effective temperature of replica $m = 0, \dots, N_{\text{rep}} - 1$, and N_{rep} is the

number of replicas. Note that each replica is run at the target temperature [i.e., $\exp(-\beta_0 E_m)$ is sampled], which makes the solute-solute and solute-solvent interactions effectively weaker in higher replicas. The corresponding acceptance formula is independent of E_{vv} , and hence a much reduced number of replicas.¹⁵ The REST has been applied recently to several biological systems with considerable success,^{18–25} but to the best of our knowledge it has not been applied to the self-assembly of dispersed monomers in solution.

The purpose of this paper is therefore to explore the utility of REST for studying supramolecular polymers in explicit solvent. For this purpose, we consider the assembly of benzene-1,3,5-tricarboxamides (BTAs)²⁶ in methylcyclohexane (MCH) solvent as a test system. The BTA consists of a benzene core with three amide groups, which form three-fold H-bonds and provide a major driving force for columnar assembly. Depending on alkyl side chains, aggregates of diverse morphology can be obtained (see Ref. 26 for a recent review). A variety of theoretical studies have also been performed for related systems.^{27–34} In the following we consider a relatively small system (10 BTA monomers dissolved in 515 MCH molecules) to facilitate extensive comparison among different methods. Nevertheless, the present system poses a significant challenge to statistical sampling because of the competition between “proper” H-bonds between stacked monomers and “improper” H-bonds via side-by-side attachment (see below). More computational details and additional data are provided in the Supplementary Material.

Conventional MD. To begin, we performed a conventional MD (cMD) calculation at 300 K. The initial state of the cMD calculation was chosen as a molecularly dispersed state.³⁵ We find that the monomers rapidly form an amorphous aggregate within ~ 20 ns. A typical MD snapshot is shown Fig. 1 (d). As seen, the random aggregate involves many “improper” H-bonds via side-by-side attachment of monomers. We continued the cMD

calculation up to 3000 ns, but the system was not able to escape from the random state and remained trapped in a meta-stable state (or a “local minimum” on the energy landscape). We repeated the same calculation with a different random seed, but the system was again trapped in a random state. The strong tendency toward amorphous aggregates is due to the relatively short alkyl side chains allowing side-by-side attachment and a rather high concentration of monomers (as typical of all-atom assembly simulations).³⁵ Fig. S3 in the Supplementary Material displays the evolution of the number of clusters in the system (denoted as N_c) at 300 K. As seen, N_c starts from ~ 10 (corresponding to a molecularly dispersed state) and rapidly decays to 1 (a single aggregate), in qualitative agreement with MD snapshots. The system then retains $N_c = 1$ or 2 for the rest of the simulation.

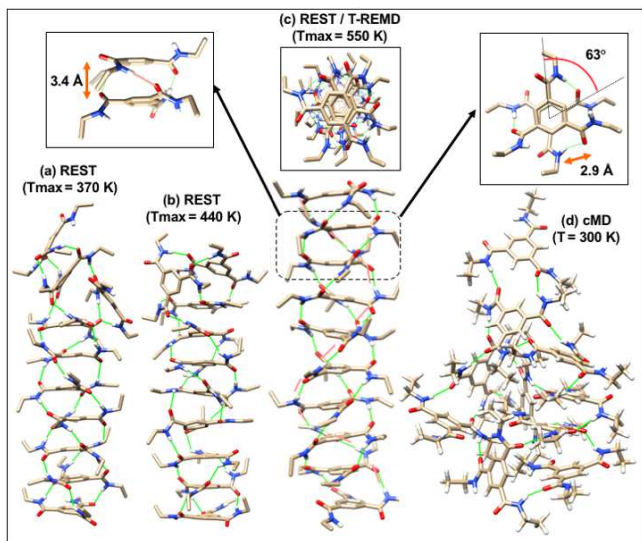


FIG. 1. Assembly structures obtained from cMD, T-REMD, and REST with different values of T_{\max} . While cMD gives an amorphous aggregate for the present system [(d)], both REST and T-REMD with $T_{\max} = 550$ K produce fully elongated BTA stacks with helical 2:1 H-bonding patterns [(c)]. See the Supplementary Material for more polymer structures obtained. When T_{\max} is lower [(a) and (b)], a few monomers are misbound to the terminal end of the polymer.

T-REMD. To avoid such kinetic trap, we next performed the T-REMD calculation to obtain a reference result. Here we set the lowest replica temperature (T_0) to 300 K (i.e., the target temperature) and the highest replica temperature (T_{\max}) to 550 K. The intermediate temperatures $\{T_m\}$ were obtained by using a web-based T-generator³⁶ and requesting an average exchange rate of 20%. This resulted in a total of 30 replicas spanning 300-550 K. The potential energy distribution of each replica shows sufficient overlap with each other,³⁵ resulting in an actual exchange rate of 20-24%. To make a fair comparison with cMD, the T-REMD calculation was performed for 100 ns per replica so that the total MD time becomes 3000 ns.

In the T-REMD method, the replica at the target temperature samples a variety of configurations with the help of higher-temperature replicas. Indeed, we find that the target replica exhibits various assembled structures ranging from a partially ordered aggregate to a fully elongated polymer. To quantify the degree of order in the system, we have calculated the length of the longest neatly stacked polymer, denoted as L_p (see the Supplementary Material for details). With the present definition, $L_p = 1$ means that no neatly stacked monomers exist in the system, while $L_p = 10$ means that the monomers form a fully elongated columnar structure. Fig. 2 (b) displays the evolution of L_p for the replica at the target temperature. It is seen that L_p takes on a wide range of values (2–10), suggesting that the canonical ensemble at 300 K is a mixture of partially ordered states (i.e., not dominated by a single long polymer).

Fig. 1 (c) displays a typical assembly structure corresponding to $L_p = 10$. Interestingly, the monomers exhibit helical 2:1 H-bonding patterns.³⁵ That is, one of the three amide hydrogens orient in one direction of the polymer (e.g., “up”), while the remaining amide hydrogens are oriented in the other direction (“down”). This H-bonding pattern agrees qualitatively with a previous theoretical study on closely related systems²⁷ and suggests that it is energetically more stable than possible 3:0 H-bonding patterns (where all the amide hydrogens are oriented in the same direction).

Fig. 2 (a) displays the evolution of L_p for the cMD calculation at 300 K. As seen, the value of L_p increases only up to 4, which corresponds to a short polymer fragment in an amorphous aggregate. The polymer does not grow further because of insufficient rearrangement of monomers within a given simulation time.

REST. We next applied the REST method to the present system. For comparison, the lowest and highest replica temperatures were chosen the same as the T-REMD calculation (i.e., $T_0 = 300$ K and $T_{\max} = 550$ K). The intermediate replica temperatures were determined by assuming a simple geometric progression³⁵ and adjusting the number of replicas (N_{rep}) to give an average exchange rate of $\sim 20\%$. This procedure resulted in $N_{\text{rep}} = 8$ and actual exchange rates of 15-22%. The effective potential energy for each replica exhibits a relatively broad distribution.³⁵ Thus, a smaller number of replicas suffice to span the same temperature range. The simulation time was set to 375 ns (per replica) to make the total MD time equal to the other calculations.

Fig. 2 (c) displays the evolution of L_p obtained from the REST calculation. As seen, the REST is also able to sample a wide range of L_p and generate fully elongated polymers with $L_p = 10$. The polymer structure thus obtained is essentially the same as shown in Fig. 1 (c). The constituent monomers also exhibit the helical 2:1 H-bonding patterns. Thus, we find that REST successfully reproduces the main feature of supramolecular polymer as obtained from T-REMD.

Some statistical data are shown in the Supplementary

Material. The distribution of the number of H-bonds and the radial distribution functions (RDFs) of benzene cores show good agreement between T-REMD and REST. On the other hand, the histogram of L_p exhibits more discrepancy between the two, suggesting that longer sampling time is necessary for better agreement. Indeed, the distribution of L_p is more difficult to converge because the present definition of L_p is rather tight³⁵ and thus it measures the formation of highly ordered structures in the system. Another factor that may affect the convergence rate of REST is the envelope-like feature of L_p observed in Fig. 2 (c), which will be discussed later.

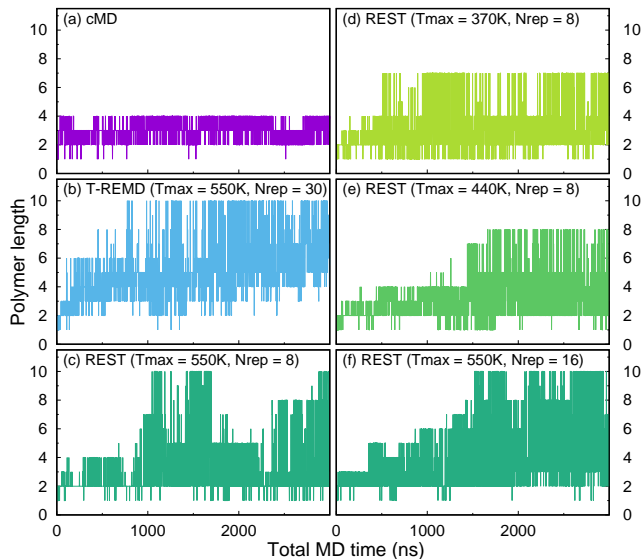


FIG. 2. Evolution of L_p (i.e., the maximum length of neatly stacked polymers) obtained from (a) cMD, (b) T-REMD, (c-f) REST calculations with different choice of T_{\max} and N_{rep} . For more details of each calculation, see Table S1 in the Supplementary Material.

REST with lower T_{\max} . The performance of replica-exchange methods is affected by many simulation parameters, and here we study the effect of T_{\max} on assembly structures. In replica-exchange simulations for biological systems, it is typical to set T_{\max} to around 400–500 K. We thus utilized somewhat lower values of T_{\max} (370 and 440 K). For simplicity, the number of replicas was chosen the same as the REST calculation above ($N_{\text{rep}} = 8$). Because of the lower T_{\max} , the effective energy distribution shows even greater overlap between adjacent replicas, resulting in a higher exchange rate on average (66 and 46 % for 370 and 440 K, respectively).³⁵

Fig. 2 (d) and (e) display the evolution of L_p obtained with lower T_{\max} . This figure shows that L_p increases only up to 7 and 8 for $T_{\max} = 370$ and 440 K, respectively. Typical polymer structures corresponding to $L_p = 7$ and 8 are displayed in Fig. 1 (a) and (b). As seen, two or three monomers bind erroneously to one terminal end of the polymer in a non-stacked manner and behave as a defect for further polymer growth. Those monomers

are not able to rearrange themselves to a neatly stacked position, i.e., “error correction” does not occur via higher replicas. Erroneous binding occurs preferentially at the terminal end (rather than the side) of a polymer, which may be due to the macrodipole of the polymer^{26,27,30} and an enhanced electrostatic field at the terminus. To make further comparison, we also performed the REST simulation with $T_{\max} = 550$ K and $N_{\text{rep}} = 16$ to obtain a greater exchange rate on average (58 %). The evolution of L_p [Fig. 2 (f)] shows that full BTA stacks with $L_p = 10$ are obtained again, indicating that the result is reproducible as long as T_{\max} is sufficiently high.

The above result suggests that the choice of T_{\max} is crucial for successful polymer elongation. This observation is consistent with the idea that T_{\max} should be high enough so that the system can overcome energy barriers for the process of interest.¹² In the present case the energy barrier arises from inter-monomer H-bonds, and the system needs to break such H-bonds via high-temperature replicas. However, the use of high T_{\max} also allows monomers to dissociate into the bulk solvent. This has both pros and cons for sampling efficiency: On one hand, the dissociation of monomers allows for partial or total “resetting” of an aggregation process at the target temperature, thus helping the system escape from local minima. On the other hand, dissociated monomers necessarily increase the entropy of the system, which is not favorable in REMD. Thus, there is some dilemma as to the choice of T_{\max} for efficient simulation.

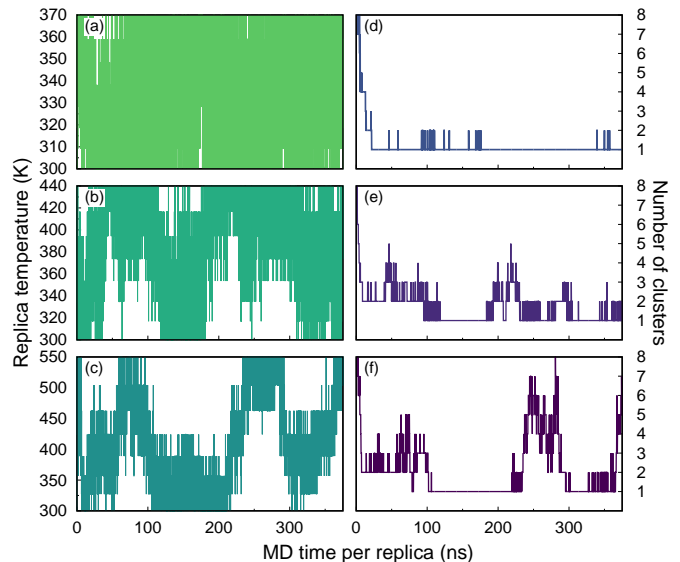


FIG. 3. Replica traversal in the temperature space for typical replicas (left panels) and the corresponding evolution of N_c (right panels) for the REST calculations. Top, middle, and bottom panels correspond to $T_{\max} = 370$, 440, and 550 K, respectively. All the simulations were performed with $N_{\text{rep}} = 8$.

Aggregation-dispersion transition and a bottle-

neck in replica temperature space. The situation can be seen more clearly by examining the replica traversal in temperature space. Fig. 3 (a) displays the evolution of temperature for a typical replica with $T_{\max} = 370$ K. The round trip occurs very rapidly between 300 and 370 K, so that the plotted curve almost fills the panel. The value of N_c for the same replica [panel (d)] starts from ~ 10 (the initial dispersed state) and decays rapidly to 1. The system then retains a single aggregate throughout the simulation (except for rare occurrence of $N_c = 2$).

When T_{\max} is raised to 440 K [panel (b)], the replica starts to show a wave-like (or envelope-like) feature in temperature space. The corresponding value of N_c indicates that the system often decomposes into several clusters. This trend becomes more evident for $T_{\max} = 550$ K [panel (c)]. Importantly, the oscillatory pattern of replica temperature is closely related to the aggregation-dispersion transition at around 400-450 K. At low replica temperatures the system retains a single aggregate, while at higher temperatures the replica makes a phase transition to a dispersed state. Once the monomers dissociate into the bulk, a certain time (20–50 ns) is necessary for the recombination to occur. This dissociation-recombination process limits the time scale of “round trips” of replicas in temperature space. The above observation is somewhat analogous to the relation between cooperative transition in proteins and the appearance of a bottleneck in temperature space.¹² That is, large temperature changes are slaved (or connected) to conformational changes in the replicas. In the present case, the dissociation and association of monomers become a limiting factor for the replica traversal between T_0 and T_{\max} .

T-REMD also exhibits a similar behavior by reflecting the aggregation-dispersion transition at 400-450 K (see the Supplementary Material). An interesting observation is that the round trips occur somewhat faster for T-REMD than REST. This is probably because the solvent is also heated in T-REMD, which facilitates the diffusion of monomers at high temperatures. This “hot solvent” effect contributes to the overall good efficiency of T-REMD despite the greater number of replicas. Nevertheless, we expect that REST will be advantageous for larger systems because of more moderate scaling of the number of replicas, which facilitates replica simulation with given parallel computational resources.³⁷

Conclusions. In this paper we have explored the utility of REST for supramolecular polymerization by using a relatively simple model in explicit solvent. For the present system, cMD has produced an amorphous aggregate and thus completely failed to predict assembly structures. On the other hand, both REST and T-REMD successfully produced a fully elongated polymer with helical H-bonding patterns. To obtain such a structure, it was necessary to raise the highest replica temperature (T_{\max}) to 550 K. This has both pros and cons on sampling efficiency, i.e., a favorable effect of allowing more active rearrangement of monomers, and an unfavorable effect of inducing aggregation-dispersion transition. While the latter was not very “sharp” for the present system and thus well tractable, it may pose a challenge for larger systems. Several approaches have been proposed to deal with such cooperative transition in REMD,³⁸ which may also prove beneficial for the present purpose.

Although all-atom self-assembly simulations are limited in both time and length scales, they are useful for providing atomistic insights into key interactions between monomers, which in turn serve as the basic information for building (or refining) coarse-grained models. We expect that REST will be useful particularly for such calculations. Applying REST to larger supramolecular systems remains a challenge for future study.

SUPPLEMENTARY MATERIAL

More computational details (with the definition of N_c and L_p); evolution of N_c for cMD at various temperatures; potential energy distribution for each replica in T-REMD and REST; additional statistical data and MD snapshots for assembly structures; replica traversal in temperature space for T-REMD; an electronic archive for the configuration and topology files of the present BTA system.

ACKNOWLEDGMENTS

The authors acknowledge support from JSPS Grant-in-Aid for Scientific Research on Innovative Areas “Dynamical ordering of biomolecular systems for creation of integrated functions” (Grant No. 25102002).

* yamamoto@kuchem.kyoto-u.ac.jp.

¹ T. F. A. de Greef and E. W. Meijer, *Nature* **453**, 171 (2008).

² T. F. A. de Greef, M. M. J. Smulders, M. Wolffs, A. P. H. J. Schenning, R. P. Sijbesma, and E. W. Meijer, *Chem. Rev.* **109**, 5687 (2009).

³ T. Aida, E. W. Meijer, and S. I. Stupp, *Science* **335**, 813 (2012).

⁴ C. Kulkarni, S. Balasubramanian, and S. J. George, *ChemPhysChem* **14**, 661 (2013).

⁵ L. Yang, X. Tan, Z. Wang, and X. Zhang, *Chem. Rev.* **115**, 7196 (2015).

⁶ S. J. Marrink and D. P. Tieleman, *Chem. Soc. Rev.* **42**, 6801 (2013).

⁷ R. C. Bernardi, M. C. R. Melo, and K. Schulten, *Biochim. Biophys. Acta* **1850**, 872 (2015).

⁸ C. Abrams and G. Bussi, *Entropy* **16**, 163 (2014).

⁹ A. J. Ballard, S. Martiniani, J. D. Stevenson, S. Somani, and D. J. Wales, *WIREs Comput. Mol. Sci.* **5**, 273 (2015).

¹⁰ U. H. E. Hansmann, *Chem. Phys. Lett.* **281**, 140 (1997).

- ¹¹ Y. Sugita and Y. Okamoto, *Chem. Phys. Lett.* **314**, 141 (1999).
- ¹² H. Nymeyer, S. Gnanakaran, and A. E. Garcia, *Methods in Enzymology* **383**, 119 (2004).
- ¹³ P. Liu, B. Kim, R. A. Friesner, and B. J. Berne, *Proc. Natl. Acad. Sci.* **102**, 13749 (2005).
- ¹⁴ X. Huang, M. Hagen, B. Kim, R. A. Friesner, R. Zhou, and B. J. Berne, *J. Phys. Chem. B* **111**, 5405 (2007).
- ¹⁵ L. Wang, R. A. Friesner, and B. J. Berne, *J. Phys. Chem. B* **115**, 9431 (2011).
- ¹⁶ T. Terakawa, T. Kameda, and S. Takada, *J. Comput. Chem.* **32**, 1228 (2011).
- ¹⁷ G. Bussi, *Mol. Phys.* **112**, 379 (2014).
- ¹⁸ C. Camilloni, D. Provasi, G. Tiana, and R. A. Broglia, *Proteins* **71**, 1647 (2008).
- ¹⁹ L. B. Wright and T. R. Walsh, *Phys. Chem. Chem. Phys.* **15**, 4715 (2013).
- ²⁰ L. Wang, Y. Deng, J. L. Knight, Y. Wu, B. Kim, W. Sherman, J. C. Shelley, T. Lin, and R. Abel, *J. Chem. Theory Comput.* **9**, 1282 (2013).
- ²¹ K. Huang and A. E. Garcia, *J. Chem. Theory Comput.* **10**, 4264 (2014).
- ²² D. J. Cole, J. Tirado-Rives, and W. L. Jorgensen, *J. Chem. Theory Comput.* **10**, 565 (2014).
- ²³ G. Stirnemann and F. Sterpone, *J. Chem. Theory Comput.* **11**, 5573 (2015).
- ²⁴ X. Pang and H. Zhou, *Biophys. J.* **109**, 1706 (2015).
- ²⁵ A. K. Smith, C. Lockhart, and D. K. Klimov, *J. Chem. Theory Comput.* **12**, 5201 (2016).
- ²⁶ S. Cantekin, T. F. A. de Greef, and A. R. A. Palmans, *Chem. Soc. Rev.* **41**, 6125 (2012).
- ²⁷ K. K. Bejagam, G. Fiorin, M. L. Klein, and S. Balasubramanian, *J. Phys. Chem. B* **118**, 5218 (2014).
- ²⁸ K. K. Bejagam and S. Balasubramanian, *J. Phys. Chem. B* **119**, 5738 (2015).
- ²⁹ K. K. Bejagam, R. C. Remsing, M. L. Klein, and S. Balasubramanian, *Phys. Chem. Chem. Phys.* **19**, 258 (2017).
- ³⁰ K. K. Bejagam, C. Kulkarni, S. J. George, and S. Balasubramanian, *Chem. Commun.* **51**, 16049 (2015).
- ³¹ M. Garzoni, M. B. Baker, C. M. A. Leenders, I. K. Voets, L. Albertazzi, A. R. A. Palmans, E. W. Meijer, and G. M. Pavan, *J. Am. Chem. Soc.* **138**, 13985 (2016).
- ³² D. Bochicchio and G. M. Pavan, *ACS Nano* **11**, 1000 (2017).
- ³³ D. Bochicchio and G. M. Pavan, *J. Phys. Chem. Lett.* **8**, 3813 (2017).
- ³⁴ I. A. W. Filot, A. R. A. Palmans, P. A. J. Hilbers, R. A. van Santen, E. A. Pidko, and T. F. A. de Greef, *J. Phys. Chem. B* **114**, 13667 (2010).
- ³⁵ See the Supplementary Material for more details.
- ³⁶ A. Patriksson and D. van der Spoel, *Phys. Chem. Chem. Phys.* **10**, 2073 (2008).
- ³⁷ See, for example, Refs. 21 and 25 for the computational cost of REST and T-REMD depending on system size.
- ³⁸ W. Zhang and J. Chen, *J. Comp. Chem.* **35**, 1682 (2014) and references therein.